Whirl-Flutter Suppression in Advanced Turboprops and Propfans by Active Control Techniques

F. Nitzsche*
Instituto Tecnológico de Aeronáutica
São José dos Campos, Brazil

Abstract

The feasibility of using the active control technique to suppress the whirl-flutter instability of advanced turboprops and propfans is analyzed. Aerodynamic vanes are incorporated at the engine nacelles to generate control airloads. The actuator system is driven by a control law derived from the linear quadratic regulator theory. The results demonstrate that the aero-servoelastic system provides enough controllability to prevent the whirl-flutter onset well beyond the design speed. The present study suggests that very efficient engine vibration isolation may be achieved by optimizing the engine-propeller suspension to attenuate unpleasant low frequencies without the risk of downgrading the required stability.

Nomenclature

$\mathbf{A}$, $\mathbf{B}$, $\mathbf{C}$ = aeroservoelatic system matrices
$A_1, \ldots A_4$ = propeller aero coefficients
a = distance between fuselage and nacelle centerlines
b = engine-propeller CG distance from pylon elastic axis
b_ε = vane semichord
$C(\kappa)$ = Theodorsen's function
c_0, c_c = blade chord, vane chord
d = propeller distance from pylon elastic axis
$\mathbb{G}$ = control gain matrix
$\mathbf{G}$ = gyroscopic loads matrix
h = pylon elastic axis out-of-plane displacement
h_y, h_z = aft fuselage cone displacement: horizontal, vertical
I_t = engine-prop mass moment-of-inertia about pylon E.A.
I_y = engine-prop-nacelle mass moment-of-inertia about pylon E.A.
I_x = total polar mass moment-of-inertia about fuselage axis
I_{ph} = propeller polar mass moment-of-inertia
J_* = cost function
J = propeller advance ratio ($=V/\Omega R$)
$\mathbf{K}$ = stiffness matrix
L_ε = vane lift
ℓ = vane distance from pylon E.A.
$\mathbf{M}$ = mass matrix
M_t = system total mass
M_ε = vane aerodynamic moment
m = engine-propeller mass
m_1 = engine-propeller-nacelle mass
m_a = $\rho(\pi c_0^2/4)R$
N = number of blades
$\mathbf{p}$ = $\mathbf{q}^*$
$\mathbb{Q}$ = output vector weighting matrix
$\mathbf{Q}^1$, $\mathbf{Q}^0$ = propeller aerodynamic damping and stiffness matrices
$\mathbf{q}$ = vector of dependent variables
$\mathbb{R}$ = control weighting matrix
$\mathbf{R}^1$, $\mathbf{R}^0$ = vane aerodynamic damping and stiffness matrices
R = propeller radius
$\mathbb{S}$ = matrix-solution of the Riccati equation
$\mathbf{S}^1$, $\mathbf{S}^2$ = aerodynamic control matrices
S_c = vane span
t = time
$\mathbf{u}$ = control vector
V = airspeed
v = horizontal displacement of engine CG w.r.t. nacelle
w = vertical displacement of engine CG w.r.t. nacelle
$\mathbf{x}$ = augmented state vector
$\mathbf{y}$ = vector of output states
γ = pylon torsion about E.A.
ε = vane rotation angle
θ = aft fuselage cone torsion
κ = reduced frequency
μ = $2N\bar{m}_a/\bar{c}_0$
ν = closed-loop control gain
ρ = air density
ϕ = engine-propeller pitch
ψ = engine-propeller yaw
ω = aeroelastic mode frequency
ω_i = engine prop uncoupled natural frequencies ($i=v, w, \psi, \phi$)
$\omega_{y,z,\theta}$ = aft fuselage uncoupled natural frequencies
$\omega_{\delta,\gamma}$ = pylon uncoupled natural frequencies
ω_a = actuator natural frequency
ζ = aeroelastic mode damping
ζ_a = actuator damping ratio
$\mathbf{1}$, $\mathbf{0}$ = unit, null matrix
$\pm$ = referred to clockwise/counter-clockwise spinning directions

Superscripts:

$*$ = $1/\Omega\ \partial/\partial t$
$-$ = dimensionless value
T = transpose
c = referred to control system
$(\ )'$ = $J^*(\ )$

Subscripts:

$1, 2$ = referred to power plants 1 and 2
a = referred to actuator
v = referred to vehicle

---

*Visiting Professor; Member AIAA.

1. Introduction

The whirl-flutter is a major aeroelastic problem described as an oscillatory instabiity of the engine-propeller installation. Two-degree-of-freedom models, for which the engine-propeller structure is considered to be a rigid body free to develop only the pitch and yaw natural modes with respect to the airstream direction, are able to reproduce the precessional motion which may become unstable under certain conditions[1]. In the classical whirl-flutter analysis, the fexibility of the system is supposed to be originated by a combination of the individual flexibilities due to both the engine suspension (or mounting system), and the back-up structure which supports it. Equivalent spring rates are determined. They provide a positive damping to the aeroelastic modes - the forward and the backward precession - up to a critical advance ratio, J^*_{cr}. Further assumptions are considered as follows: (1) uniform flow reaching the propeller disk; (2) small-perturbation, two-dimensional, blade section aerodynamic theory; (3) no significant motion of the engine-propeller center-of-mass; (4) no coupling between the engine-propeller whirl modes and the natural modes associated with the back-up structure. Furthermore, by definition, in a whirl-flutter formulation the airloads are solely generated by the propeller motion relative to the airstream. However, more sophisticated idealizations have demonstrated that the aforementioned hypotheses are not always representative. Significant motion of the engine-propeller CG is verified in complex engine-suspension systems, specially when the distance between the elastic center and the mass center is not negligible, and yields highly coupled natural modes involving not only the angular displacements of the power plant (pitch-yaw), but also the linear displacements (vertical-horizontal) of the same with respect to the unperturbed flow. In general, both the roll and the fore-and-aft motions of the engine-propeller setup have no participation in the whirl-flutter phenomenon[2]. Zwaan and Bergh have also demonstrated that the wing natural modes may couple with the engine-propeller whirl modes to modify the aeroelastic behavior of the system[3]. Hence, in modern configurations of turboprops, in which two pusher propeller engines are supported by short pylons cantilivered with the aft fuselage cone, the whirl-flutter analysis requires some more elaborate work. Under the dynamic point-of-view, this problem was treated in two former papers[4,5]. A sketch of the 15-degree-of-freedom model used to investigate the problem is reproduced in Fig.1 for the sake of completeness. Considerable influence of the back-up structure dynamics was observed in the stability characteristics. The whirl modes developed by the two power plants presented strong coupling with the natural modes of the back-up structure. Both symmetric and antisymmetric whirl-flutter conditions were verified, involving in many cases a *major* participation of the supporting structure motion rather than the classical engine-propeller-nacelle precessional modes. Situations such as the relative spinning direction of the two propellers could be investigated as well, demonstrating that counter-rotating propellers lead to larger whirl-flutter margins.

Aside from that, in advanced turbopropeller configurations, another problem must be addressed: the influence of the nonuniform flow induced on the propeller disk by the entire aircraft, specially by the pylons which support the engines. The uniform flow is one of the basic hypotheses of the classical solution. However, if a steady flow perturbation is assumed, the problem may be solved by well known techniques. For an observer sitting on the reference frame fixed with respect to the propeller blade, the peturbation flow field generated by the aircraft is periodic. The periodic aerodynamic loads may be added to the classical aerodynamic loads, due to the propeller motion with respect to the *uniform* flow, if the assumption of small angles is preserved. The transition matrix over a complete characteristic period may be calculated and Floquet's theory for the stability of periodic systems may be used to check the whirl-flutter margin[6]. On the other hand, if short, multiple, plate-like blades are employed, as in propfan installations, even the classical whirl-flutter aerodynamic theory used for propeller blades should be modified to introduce the cascade effects[7].

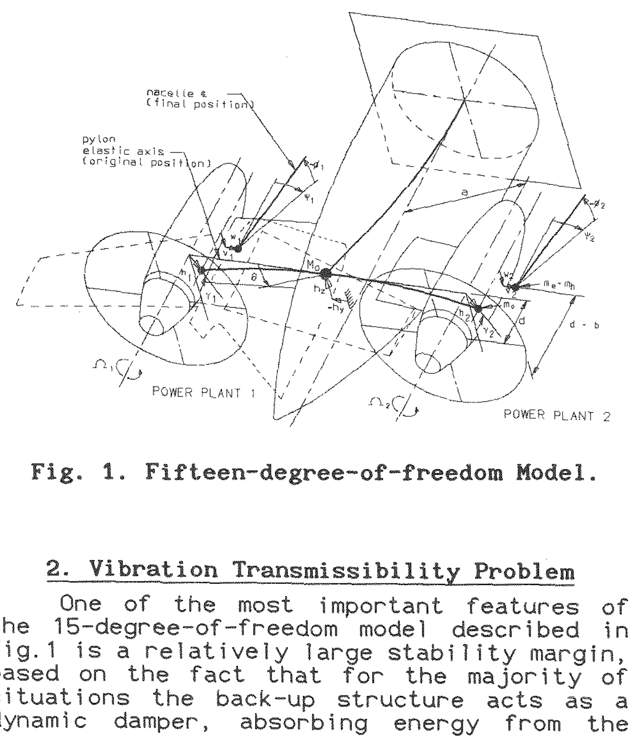

Fig. 1. Fifteen-degree-of-freedom Model.

2. Vibration Transmissibility Problem

One of the most important features of the 15-degree-of-freedom model described in Fig.1 is a relatively large stability margin, based on the fact that for the majority of situations the back-up structure acts as a dynamic damper, absorbing energy from the engine mounting system[4]. Therefore, it is feasible to consider the back-up structure as an integrated part of the design of the engine vibration isolation and, while keeping the whirl-flutter stability, to reduce the transmissibility levels. Figure 2 depicts a typical whirl-flutter stability contour for the critical advance ratio J^*_{cr} as function of the engine suspension system uncoupled, dimensionless, natural frequencies in pitch and yaw, ($\bar{\omega}_\phi$ and $\bar{\omega}_\psi$ respectively). The shaded regions correspond to islands of high stability, where the engine vibration transmissibility optimization may be potentially explored. However, if passenger comfort allied to the high speed are the primary design objectives, it represents a step further to apply the active control technology to prevent the onset of whirl-flutter. As a result, the engine suspension system may be designed as soft as possible to cut-off the unpleasant, low frequency, vibration spectrum inherent to turbopropellers. The present work investigates the possibility of obtaining higher whirl-flutter critical speeds by exploring the advantage, under the control point-of-view, of having a multi-degree-of-freedom dynamic system with strongly coupled eigenvectors.

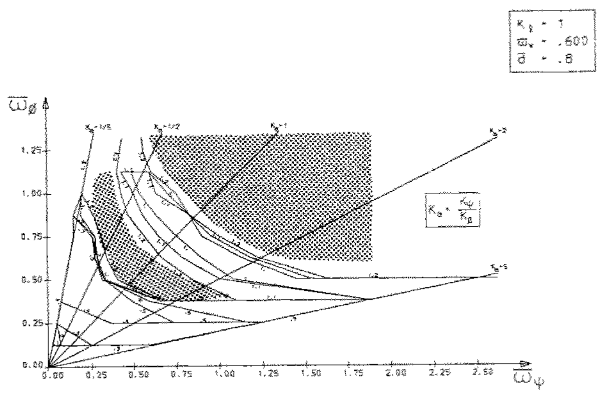

Fig. 2. Whirl-Flutter Stability Contours for the Dimensionless Advance Ratio J^* as a Function of the Engine Suspension Uncoupled Dimensionless Natural Frequencies in Pitch and Yaw.

3. Open-Loop Model

The open loop model is described in reference 4. The 15-degree-of-freedom linear, coupled, second order differential equations are cast in state vector form:

$$\overset{*}{\mathbf{x}}_v = \mathbf{A}_v\, \mathbf{x}_v \tag{1}$$

where:

$$\mathbf{x}_v = \lfloor\, \mathbf{p} \quad \mathbf{q} \,\rfloor^T \tag{2}$$

$$\mathbf{p} = \overset{*}{\mathbf{q}} \tag{3}$$

$$\mathbf{A}_v = \begin{bmatrix} \mathbf{M}^{-1}(\mu Q^1 - G) & \mathbf{M}^{-1}(\mu Q^0 - K) \\ 1 & 0 \end{bmatrix} \tag{4}$$

and

$$\mathbf{q} = \lfloor\, \psi_1\ \bar{v}_1\ \bar{h}_y\ \bar{v}_2\ \psi_2 \mid \phi_1\ \gamma_1\ \bar{h}_1\ \bar{w}_1\ \bar{h}_z\ \theta\ \bar{w}_2\ \bar{h}_2\ \gamma_2\ \phi_2 \,\rfloor^T \tag{5}$$

is the vector collecting the dependent variables of the problem. The matrices **M**, **G**, **K**, $\mathbf{Q}^1$ and $\mathbf{Q}^0$ are defined in Apendix A. They are function of the mass, stiffness and geometric properties of the dynamic system along with the flight and engine operating conditions. A thoroughly discussion on the characteristics of the above defined aeroelastic problem is presented in references 4 and 5. Here, it is important to stress the highly coupled nature of the complex eigenvectors associated with the aeroelastic modes, indicating that the studied aircraft configuration whirl-flutters in a complicated pattern, involving many components of the back-up structure: pylon bending-torsion and fuselage bending-torsion. The instability associated with a complex eigenvector having the main component related to a back-up structure displacement, generally denominated *whirl-induced-flutter* in reference 4, will be the matter of primary interest of this work.

4. Aeroservoelastic Model

To achieve the controllability of the open-loop system, a pair of aerodynamic vanes is designed for the two naceles and positioned at a distance ℓ from the pylon elastic axes (Fig.3). The goal is to provide through appropriate rotations of the two vanes the aerodynamic forces which can control both the pylon bending and the pylon torsion in symmetric and antisymmetric whirl-flutter modes.

The aerodynamic loads (lift and moment) are obtained from Theodorsen's unsteady theory for incompressible flow[8], which may be adjusted for compressibility and three-dimensional effects. Assuming that the vanes are driven by an actuator system connected to the 1/4-chord position, from Fig.4 one has for the two-degree-of-freedom aerodynamic problem:

$$L_\varepsilon = \rho b_\varepsilon^2(\ V\pi(\dot{\varepsilon}-\dot{\gamma})\ ) + 2\pi\rho V b_\varepsilon C(\kappa)(\ V(\varepsilon-\gamma) + (\dot{h}-\dot{h}_z \pm \dot{\theta} a) + b_\varepsilon(\dot{\varepsilon}-\dot{\gamma})/4\ ) \tag{6}$$

$$M_\varepsilon = -\rho b_\varepsilon^3 V\pi(\dot{\varepsilon}-\dot{\gamma})/4 \tag{7}$$

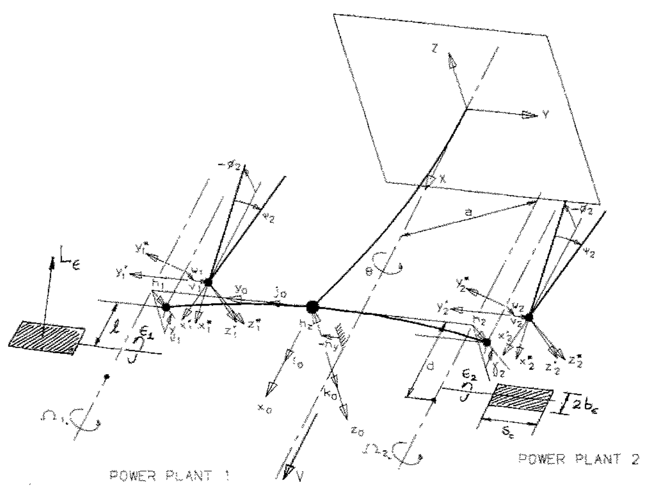

Fig. 3. Aerodynamic Vanes Geometric Definition.

where, in the term $\pm\dot{\theta}a$, the plus sign is associated with the propeller #1 and the minus sign with the propeller #2. In these equations the apparent mass is neglected. Furthermore, a quasi-steady approximation is coherent with the aerodynamic theory developed for the propeller blades. Hence, the Theodorsen's lift deficiency function is identified to the unity for all values of reduced frequency.

Next, Eqs.(6) and (7) are put in a dimensionless state vector form compatible with the open-loop problem described in reference 4 and the new generalized forces are included in the equations of motion. The original aeroelastic equations, augmented with the four new states represented by the rotation of the two vanes, are rewritten as:

$$\overset{*}{\mathbf{x}} = \mathbf{A\,x} + \mathbf{B\,u} \tag{8}$$

where:

$$\mathbf{x} = \lfloor \mathbf{x}_v \quad \mathbf{x}_a \rfloor^T \tag{9}$$

$$\mathbf{u} = \lfloor \varepsilon_1^c \quad \varepsilon_2^c \rfloor^T \tag{10}$$

$$\mathbf{A} = \begin{bmatrix} \mathbf{A}_v^{new} & \mathbf{B}_v \\ \mathbf{0} & \mathbf{A}_a \end{bmatrix} \tag{11}$$

$$\mathbf{A}_v^{new} = \begin{bmatrix} \mathbf{M}^{-1}(\mu(\mathbf{Q}^1+\mathbf{R}^1)-\mathbf{G}) & \mathbf{M}^{-1}(\mu(\mathbf{Q}^0+\mathbf{R}^0)-\mathbf{K}) \\ \mathbf{1} & \mathbf{0} \end{bmatrix} \tag{12}$$

$$\mathbf{B}_v = \begin{bmatrix} \mathbf{M}^{-1}\mu\mathbf{S}^1 & \mathbf{M}^{-1}\mu\mathbf{S}^1 \\ 0 & 0 \end{bmatrix} \tag{13}$$

$$\mathbf{B} = \begin{bmatrix} 0 \\ \mathbf{B}_a \end{bmatrix} \tag{14}$$

$$\mathbf{x}_a = \lfloor \overset{*}{\varepsilon}_1 \; \overset{*}{\varepsilon}_2 \; \varepsilon_1 \; \varepsilon_2 \rfloor^T \tag{15}$$

The aerodynamic matrices $\mathbf{R}^1$, $\mathbf{R}^0$, $\mathbf{S}^1$ and $\mathbf{S}^0$, associated with the generalized airloads developed by the vanes, along with $\mathbf{A}_a$ and $\mathbf{B}_a$, describing the dynamics of the control system, are presented in Appendix B.

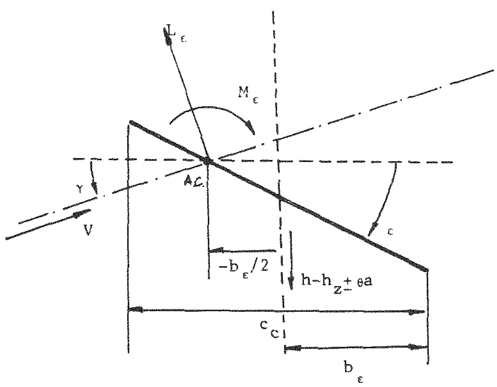

Fig. 4. Control Vane Aerodynamics.

5. Control Law Synthesis

Optimal regulator theory, which provides the minimization of a quadratic cost function of both the system states and the control, subject to the aeroservoelastic equations of motion, will be employed to determine the control law. Hence, the problem is posed as:

$$\min_{u} J = \int_0^{\infty} (\, \mathbf{y}^T\mathbb{Q}\,\mathbf{y} + \mathbf{u}^T\mathbb{R}\,\mathbf{u}\,)\, d\bar{t} \tag{16}$$

$$\text{STO: } \overset{*}{\mathbf{x}} = \mathbf{A\,x} + \mathbf{B\,u} \tag{17}$$

$$\mathbf{y} = \mathbf{C\,x} \tag{18}$$

The solution of the latter problem is given by the LQR (linear quadratic regulator) theory[9]. The full-state feedback control law is:

$$\mathbf{u} = -\mathbb{G}\,\mathbf{x} \tag{19}$$

which, for the constant-coefficient differential equations, is derived from the steady state solution of the Riccati equation:

$$\mathbb{G} = \mathbb{R}^{-1}\mathbf{B}^T\,\mathbb{S} \tag{20}$$

where:

$$\mathbb{S}\,\mathbf{A} + \mathbf{A}^T\mathbb{S} + \mathbf{C}^T\mathbb{Q}\,\mathbf{C} - \mathbb{S}\,\mathbf{B}\,\mathbb{R}^{-1}\mathbf{B}^T\mathbb{S} = 0 \tag{21}$$

6. Whirl-Flutter Stability. Closed-Loop.

The matrices $\mathbb{Q}$ and $\mathbb{R}$ in Eq.(16) are respectively weighting the output and control vectors. Both are chosen to be unit matrices in the present solution. In general, $\mathbb{R}$ is written as $\mathbb{R} = \nu\,\mathbf{1}$, where ν is the control gain of the closed-loop system. Here, ν is implicit in the matrix equations, and may be associated with the ratio:

$$\nu = c_c S_c/(N\, c_0 R) \tag{22}$$

which gives the area of the control vanes over the total area of the propeller blades. The ratio ν may be tuned to match the desired overall feedback control gain at the design point J^*_{des}.

The parameters chosen in the present study to represent the aeroservoelastic system are collected in Table 1. The corresponding free-vibration eigenvalues are given in Table 2. Figure 5 depicts the root-locus plot of the open-loop eigenvalues of the characteristic matrix $\mathbf{A}$ as a function of the advance ratio J^* at sea-level condition. The whirl- flutter onset occurs at $J^*=1.15$. Referring to the phase diagram of the associated free- vibration eigenvector, the unstable mode presents a significant motion of the pylon, and should be controllable by the proposed control system. In Fig.7, the result of using a LQR algorithm to determine the optimal control gain at $J^*_{des} = 1.5$ is shown. The root- locus plot versus J^* of the closed-loop system characteristic matrix, $(\mathbf{A}-\mathbf{B}\mathbb{G})$, demonstrates that whirl-flutter is precluded in the entire range of J^* values. In fact, the former instability was no longer verified up to J^* = 2.0. Furthermore, the complex eigenvalues present large damping ratios, well beyond the desired design point. It is well-known that the LQR theory does not guarantee that the aeroservoelastic system is also free from the static (divergence) instability *below* the design point[10]. However, the pusher configuration is known to be intrinsically free from divergence. A second example demonstrates that even with the output matrix C constructed to select only those entries corresponding to the states associated with the pylon bending-torsion, the system is controllable with an ample margin (Fig.8).

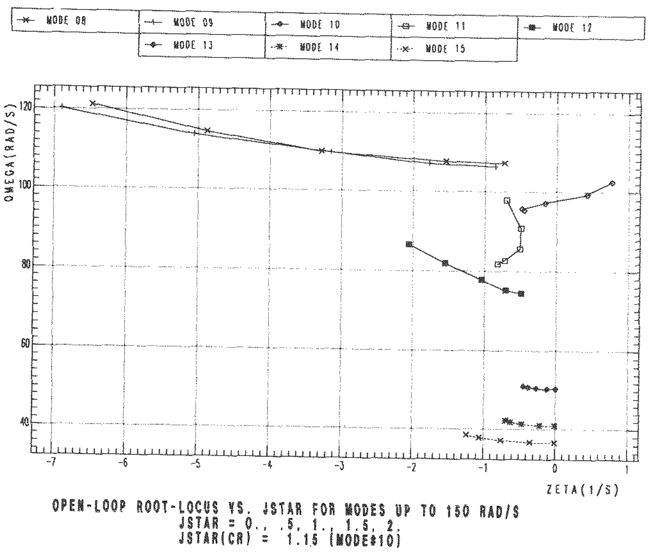

Fig. 5. Open-Loop Root-Locus vs. J^*

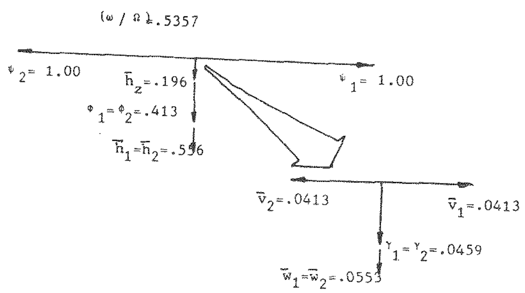

Fig. 6. Phase Diagram - Critical Free-Vibration Open-Loop Eigenmode: Backward Elliptical Precession for the two Counter-rotating Propellers (clock/counter-clockwise spinning direction), symmetric pylon bending-torsion and fuselage vertical bending out-of-phase w.r.t. pylon motion.

Table 1: Definition of the Aeroservoelastic System.

$\bar{a}$ = 1.6216
$\bar{b}$ = .2008
$\bar{d}$ = .7876
$\bar{c}_0$ = .1961
$\bar{c}_c$ = .2317
ν = .0760
$\bar{r}$ = .3861
μ = .0013
Ω = 178 rad/s
$a_1^{(1)} = a_2^{(1)}$ = .4000
$a_1^{(0)} = a_2^{(0)}$ = 4.000
$b_1^{(0)} = b_2^{(0)}$ = 4.000
$\Omega_1 > 0$, $\Omega_2 < 0$
$\bar{m}$ = .1353
$\bar{m}_0$ = .0109
$\bar{I}_t$ = .0355
$\bar{I}_y$ = .0390
$\bar{I}_x$ = 1.030
$\bar{I}_{ph}$ = .0033
$\bar{\omega}_{\psi 1} = \bar{\omega}_{\psi 2}$ = .3186
$\bar{\omega}_{\phi 1} = \bar{\omega}_{\phi 2}$ = .2167
$\bar{\omega}_{v1} = \bar{\omega}_{v2} = \bar{\omega}_{w1} = \bar{\omega}_{w2}$ = 1.681
$\bar{\omega}_{\gamma}$ = 1.796
$\bar{\omega}_{\delta}$ = .1685
$\bar{\omega}_{y}$ = .0823
$\bar{\omega}_{z}$ = .0628
$\bar{\omega}_{\theta}$ = .0600

Table 2: Aeroservoelastic Open-Loop System: Free-vibration Eigenvalues: J^* =0; ρ = 0; Ω = 178 rad/s, counter-rotating propellers.

mode number	ω/Ω	ζ/Ω
01	4.9928	0
02	4.9888	0
03	4.6721	0
04	4.6721	0
05	1.6400	0
06	1.4346	0
07	.9300	0
08	.6027	0
09	.5981	0
10	.5357	0
11	.4598	0
12	.4157	0
13	.2828	0
14	.2298	0
15	.2053	0
16*	1.990	-.200
17*	1.990	-.200

*control system eigenvalues

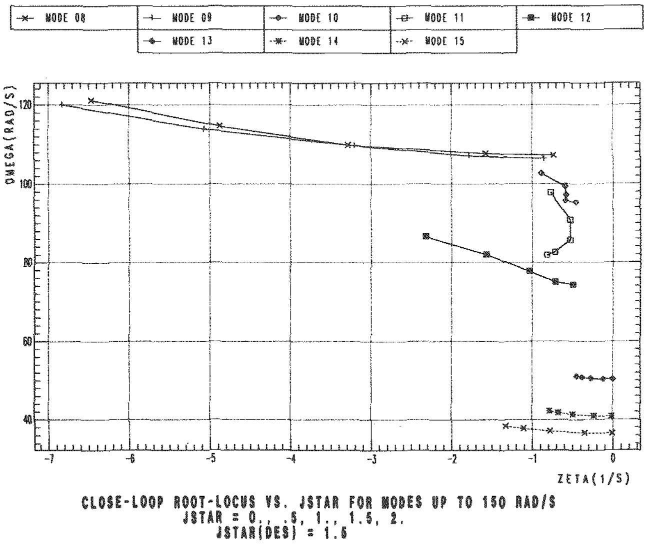

Fig. 7. Closed-Loop Root-Locus vs J^*: full-state output matrix. C = 1.

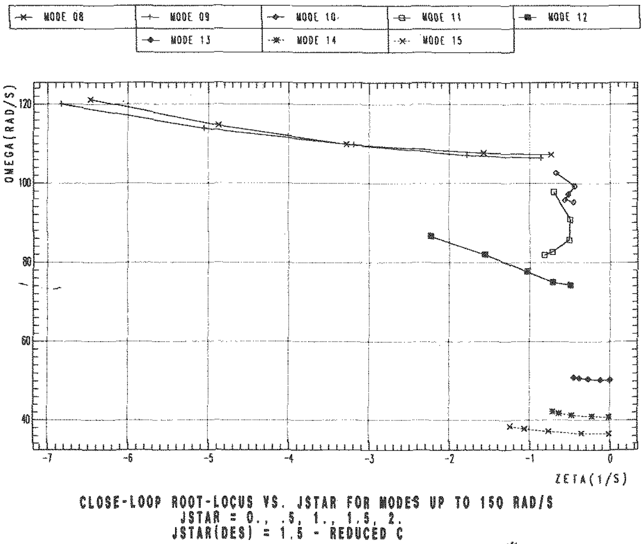

Fig. 8. Closed-Loop Root-Locus vs J^*: reduced output matrix for pylon motion alone.

7. Conclusions

The present work confirms that the active control technique may be used to prevent the whirl-flutter onset. The reason for the particularly good results achieved with the proposed control system, lies on the great controllability of the aeroelastic system due to the strong dynamic coupling observed in the whirl modes. This situation is likely to be inherent to advanced turboprop and propfan configurations. The ability of suppressing the instability onset up to very high speeds using a relatively simple control system, based on aerodynamic vanes attached to the nacelles, opens a vast new area of promising research. The problem of vibration attenuation, specially critical in propeller-driven aircrafts, may be more efficiently solved if the possibility of designing unusually soft engine suspension systems which do not become unstable at low speeds is visualized.

Apendix A: Open-Loop Matrices

$$M=\begin{bmatrix} M_{11} & 0 \\ 0 & M_{22} \end{bmatrix} \quad G=\begin{bmatrix} 0 & -G_{21}^T \\ G_{21} & 0 \end{bmatrix} \quad K=\begin{bmatrix} K_{11} & 0 \\ 0 & K_{22} \end{bmatrix}$$

$$Q^1=\begin{bmatrix} Q_{11}^1 & Q_{21}^{1\,T} \\ Q_{21}^1 & Q_{22}^1 \end{bmatrix} \qquad Q^0=\begin{bmatrix} Q_{11}^0 & -Q_{21}^{0\,T} \\ Q_{21}^0 & Q_{22}^{0\,T} \end{bmatrix}$$

$$M_{11}=\begin{bmatrix} I_t & \bar{s}_\gamma & -\bar{s}_\gamma & 0 & 0 \\ & \bar{m} & -\bar{m} & 0 & 0 \\ & & 1 & -\bar{m} & -\bar{s}_\gamma \\ & \text{sym} & & \bar{m} & \bar{s}_\gamma \\ & & & & I_t \end{bmatrix}$$

$$M_{22}=\begin{bmatrix} I_t & I_t & -\bar{s}_\gamma & -\bar{s}_\gamma & \bar{s}_\gamma & -\bar{s}_{\gamma\theta} & 0 & 0 & 0 & 0 \\ & I_y & -\bar{s}_\gamma & -\bar{s}_\gamma & \bar{s}_\gamma & -\bar{s}_{\gamma\theta} & 0 & 0 & 0 & 0 \\ & & \bar{m}_1 & \bar{m} & -\bar{m}_1 & \bar{s}_\theta & 0 & 0 & 0 & 0 \\ & & & \bar{m} & -\bar{m} & \bar{a}\bar{m} & 0 & 0 & 0 & 0 \\ & & & & 1 & 0 & -\bar{m} & -\bar{m}_1 & \bar{s}_\gamma & \bar{s}_\gamma \\ & & & & & I_x & -\bar{a}\bar{m} & -\bar{s}_\theta & \bar{s}_{\gamma\theta} & \bar{s}_{\gamma\theta} \\ & & \text{sym} & & & & \bar{m} & \bar{m} & -\bar{s}_\gamma & -\bar{s}_\gamma \\ & & & & & & & \bar{m}_1 & -\bar{s}_\gamma & -\bar{s}_\gamma \\ & & & & & & & & I_y & I_t \\ & & & & & & & & & I_t \end{bmatrix}$$

$$G_{21}=\begin{bmatrix} \pm I_{ph} & 0 & \dots & 0 \\ \pm I_{ph} & 0 & \dots & 0 \\ 0 & 0 & \dots & 0 \\ \dots & & & \\ 0 & 0 & \dots & \pm I_{ph} \\ 0 & 0 & \dots & \pm I_{ph} \end{bmatrix} \quad K_{11}=\begin{bmatrix} I_t\bar{\omega}_{\psi 1}^2 & & & & \\ & \bar{m}\omega_{v1}^2 & & & \\ & & \bar{\omega}_y^2 & & \\ & & & \bar{m}\omega_{v2}^2 & \\ & & & & I_t\bar{\omega}_{\psi 2}^2 \end{bmatrix}$$

$$K_{22}=\begin{bmatrix} I_t\bar{\omega}_{\phi 1}^2 & & & & & & & & & \\ & I_y\bar{\omega}_\gamma^2 & & & & & & & & \\ & & \bar{m}_1\bar{\omega}_\delta^2 & & & & & & & \\ & & & \bar{m}\omega_{w1}^2 & & & & & & \\ & & & & \bar{\omega}_z^2 & & & & & \\ & & & & & I_x\bar{\omega}_\theta^2 & & & & \\ & & & & & & \bar{m}\omega_{w2}^2 & & & \\ & & & & & & & \bar{m}_1\bar{\omega}_\delta^2 & & \\ & & & & & & & & I_y\bar{\omega}_\gamma^2 & \\ & & & & & & & & & I_t\bar{\omega}_{\phi 2}^2 \end{bmatrix}$$

$$Q_{11}^1=\begin{bmatrix} -A_4 & -\bar{d}A_1 & \bar{d}A_1 & 0 & 0 \\ & -A_1 & A_1 & 0 & 0 \\ & & -2A_1 & A_1 & \bar{d}A_1 \\ & \text{sym} & & -A_1 & -\bar{d}A_1 \\ & & & & -A_4 \end{bmatrix}$$

$$
Q^1_{21}=\begin{bmatrix}
0 & \mp A_2 & \pm A_2 & 0 & 0\\
0 & \mp A_2 & \pm A_2 & 0 & 0\\
\mp A_2 & 0 & 0 & 0 & 0\\
\mp A_2 & 0 & 0 & 0 & 0\\
\pm A_2 & 0 & 0 & 0 & \pm A_2\\
\mp A_2 & 0 & 0 & 0 & \pm A_2\\
0 & 0 & 0 & 0 & \mp A_2\\
0 & 0 & 0 & 0 & \mp A_2\\
0 & 0 & \pm A_2 & \mp A_2 & 0\\
0 & 0 & \pm A_2 & \mp A_2 & 0
\end{bmatrix}
$$

$$
Q^1_{22}=\begin{bmatrix}
-A_4 & -A_4 & \bar{d}A_1 & \bar{d}A_1 & -\bar{d}A_1 & \bar{a}\bar{d}A_1 & 0 & 0 & 0 & 0\\
 & -A_4 & \bar{d}A_1 & \bar{d}A_1 & -\bar{d}A_1 & \bar{a}\bar{d}A_1 & 0 & 0 & 0 & 0\\
 & & -A_1 & -A_1 & A_1 & -\bar{a}A_1 & 0 & 0 & 0 & 0\\
 & & & -A_1 & A_1 & -\bar{a}A_1 & 0 & 0 & 0 & 0\\
 & & & & -2A_1 & 0 & A_1 & A_1 & -\bar{d}A_1 & \bar{d}A_1\\
 & & & & & -2\bar{a}^2A_1 & \bar{a}A_1 & \bar{a}A_1 & -\bar{a}\bar{d}A_1 & -\bar{a}\bar{d}A_1\\
 & & & & & & -A_1 & -A_1 & \bar{d}A_1 & \bar{d}A_1\\
 & \text{sym} & & & & & & -A_1 & \bar{d}A_1 & \bar{d}A_1\\
 & & & & & & & & -A_4 & -A_4\\
 & & & & & & & & & -A_4
\end{bmatrix}
$$

$$
Q^0_{11}=\begin{bmatrix}
-\bar{d}A'_1 & 0 & \dots & 0\\
-A'_1 & 0 & \dots & 0\\
A'_1 & 0 & \dots & A'_1\\
0 & 0 & \dots & -A'_1\\
0 & 0 & \dots & -\bar{d}A'_1
\end{bmatrix}
\qquad
Q^0_{21}=\begin{bmatrix}
\pm A'_2 & 0 & \dots & 0\\
\pm A'_2 & 0 & \dots & 0\\
0 & 0 & \dots & 0\\
\dots & & & \\
0 & 0 & \dots & \pm A'_2\\
0 & 0 & \dots & \pm A'_2
\end{bmatrix}
$$

$$
Q^0_{22}=\begin{bmatrix}
-\bar{d}A'_1 & -\bar{d}A'_1 & 0 & \dots & & 0\\
-\bar{d}A'_1 & -\bar{d}A'_1 & 0 & \dots & & 0\\
A'_1 & A'_1 & 0 & \dots & & 0\\
A'_1 & A'_1 & 0 & \dots & & 0\\
-A'_1 & -A'_1 & 0 & \dots & -A'_1 & -A'_1\\
\bar{a}A'_1 & \bar{a}A'_1 & 0 & \dots & -\bar{a}A'_1 & -\bar{a}A'_1\\
0 & \dots & & & A'_1 & A'_1\\
0 & \dots & & & A'_1 & A'_1\\
0 & \dots & & & -\bar{d}A'_1 & -\bar{d}A'_1\\
0 & \dots & & & -\bar{d}A'_1 & -\bar{d}A'_1
\end{bmatrix}
$$

where:

$$\bar{s}_\gamma = \overline{bm} \qquad \bar{s}_\theta = \overline{am}_1 \qquad \bar{s}_{\gamma\theta} = \overline{abm}$$

and

$$A_1 = J^{*2}\ln\left[(1+\beta)/J^*\right]$$
$$A_2 = 1/2J^*(\beta-A_1)$$
$$A_3 = 1/4(\beta-3J^*A_2)$$
$$A_4 = \bar{d}^2A_1+A_3$$
$$\beta = \mathrm{sqrt}(1+J^{*2})$$

The geometric parameters are adimensionalized by R, the mass parameters by M_t, the mass moment-of-inertia parameters by M_tR^2 and the frequencies by Ω.

Apendix B: Closed-Loop Matrices

$$
R^{0,1}=\begin{bmatrix} 0 & 0\\ 0 & R^{0,1}_{22}\end{bmatrix}
\qquad
S^{0,1}=\begin{bmatrix} 0\\ S^{0,1}_2\end{bmatrix}
$$

$$
R^1_{22}=\begin{bmatrix}
0 & 0 & 0 & 0 & 0 & 0 & 0 & 0 & 0 & 0\\
0 & \bar{r}_{77} & \bar{r}_{78} & 0 & -\bar{r}_{78} & \overline{ar}_{78} & 0 & 0 & 0 & 0\\
0 & \bar{r}_{87} & \bar{r}_{88} & 0 & -\bar{r}_{88} & \overline{ar}_{88} & 0 & 0 & 0 & 0\\
0 & 0 & 0 & 0 & 0 & 0 & 0 & 0 & 0 & 0\\
0 & -\bar{r}_{87} & -\bar{r}_{88} & 0 & 2\bar{r}_{88} & 0 & 0 & -\bar{r}_{88} & -\bar{r}_{87} & 0\\
0 & \overline{ar}_{87} & \overline{ar}_{88} & 0 & 0 & 2\bar{a}^2\bar{r}_{88} & 0 & -\overline{ar}_{88} & -\overline{ar}_{87} & 0\\
0 & 0 & 0 & 0 & 0 & 0 & 0 & 0 & 0 & 0\\
0 & 0 & 0 & 0 & -\bar{r}_{88} & -\overline{ar}_{88} & 0 & \bar{r}_{88} & \bar{r}_{87} & 0\\
0 & 0 & 0 & 0 & -\bar{r}_{78} & -\overline{ar}_{78} & 0 & \bar{r}_{78} & \bar{r}_{77} & 0\\
0 & 0 & 0 & 0 & 0 & 0 & 0 & 0 & 0 & 0
\end{bmatrix}
$$

$$
R^0_{22}=\begin{bmatrix}
0 & 0 & 0 & \dots & 0 & 0\\
0 & -\bar{r}'_{78} & 0 & \dots & 0 & 0\\
0 & -\bar{r}'_{88} & 0 & \dots & 0 & 0\\
0 & 0 & 0 & \dots & 0 & 0\\
0 & \bar{r}'_{88} & 0 & \dots & -\bar{r}'_{88} & 0\\
0 & -\overline{ar}'_{88} & 0 & \dots & \overline{ar}'_{88} & 0\\
0 & 0 & 0 & \dots & 0 & 0\\
0 & 0 & 0 & \dots & -\bar{r}'_{88} & 0\\
0 & 0 & 0 & \dots & -\bar{r}'_{78} & 0\\
0 & 0 & 0 & \dots & 0 & 0
\end{bmatrix}
$$

$$
S^1_2=\begin{bmatrix}
0 & 0\\
-\bar{r}_{77} & 0\\
-\bar{r}_{87} & 0\\
0 & 0\\
\bar{r}_{87} & \bar{r}_{87}\\
-\overline{ar}_{87} & \overline{ar}_{87}\\
0 & 0\\
0 & -\bar{r}_{87}\\
0 & -\bar{r}_{77}\\
0 & 0
\end{bmatrix}
\qquad
S^0_2=\begin{bmatrix}
0 & 0\\
\bar{r}'_{78} & 0\\
\bar{r}'_{88} & 0\\
0 & 0\\
-\bar{r}'_{88} & \bar{r}'_{88}\\
\overline{ar}'_{88} & -\overline{ar}'_{88}\\
0 & 0\\
0 & \bar{r}'_{88}\\
0 & \bar{r}'_{78}\\
0 & 0
\end{bmatrix}
$$

$$
A_a=\begin{bmatrix}
-a_1^{(1)} & 0 & -a_1^{(0)} & 0\\
0 & -a_2^{(1)} & 0 & -a_2^{(0)}\\
1 & 0 & 0 & 0\\
0 & 1 & 0 & 0
\end{bmatrix}
\qquad
B_a=\begin{bmatrix}
b_1^{(0)} & 0\\
0 & b_2^{(0)}\\
0 & 0\\
0 & 0
\end{bmatrix}
$$

where:

$$\bar{r}_{77} = -1/2J^*\bar{c}_c\nu\ (3\bar{l}+1/2c_c)$$
$$\bar{r}_{78} = 2J^*\nu\ \bar{l}$$
$$\bar{r}_{87} = 3/2J^*\nu\ \bar{c}_c$$
$$\bar{r}_{88} = -2J^*\nu$$

$$a^{(1)} = 2\zeta_a\omega_a/\Omega \qquad a^{(0)}=(\omega_a/\Omega)^2 \qquad b^{(0)}=(\omega_a/\Omega)^2$$

References

[1]Houbolt, J.C. and Reed, W.H., III, "Propeller-Nacelle Whirl-Flutter, "*J. of the Aerospace Sciences*, 29(3):333-346, March 1962.

[2]Resende, H.B., "Estudos na Análise de Whirl-Flutter,"M.S. Dissertation, Instituto Tecnológico de Aeronáutica, CTA, São José dos Campos Brazil, 1987.

[3]Zwaan, R.J. and Bergh, H.,"Restricted Report F.228,"National Aeronautical Research Institute, NLR, The Netherlands, February 1962.

[4]Nitzsche, F.,"Whirl Flutter Investigation on an Advance Turboprop Configuration," *J. of Aircraft*, 26(10): 939-946, October 1989.

[5]Nitzsche, F.,"Insights on the Whirl-Flutter Phenomena of Advanced Turboprops and Propfans," AIAA Paper No. 89-1235, April 1989.

[6]Nitzsche, F. and Rodrigues, E.A.,"Whirl-Flutter Stability of a Pusher Configuration Subject to a Nonuniform Flow," AIAA Paper No. 90-1162, April 1990.

[7]Bendiksen, O.,"Aeroelastic Problems in Turbomachines," AIAA Paper No. 90-1157, April 1990.

[8]Theodorsen, T. and Garrick, I.E., "Non-Stationary Flow about a Wing-Aileron-Tab Combination Including Aerodynamic Balance," NACA Report 736, 1942.

[9]Kwakernaak, H. and Sivan, R., *Linear Optimal Control Systems*, John Wiley & Sons, New York, 1972, Ch. 3.

[10]Zeiler, T.A. and Weisshaar, T.A., "Integrated Aeroservoelastic Tailoring of Lifting Surfaces,"*J.of Aircraft*, 25(1):76-83, January 1988.